Effect of Membrane Composition on Antimicrobial Peptides Aurein 2.2 and 2.3 From Australian Southern Bell Frogs

John T. J. Cheng,[†] John D. Hale,[‡] Melissa Elliot,[‡] Robert E. W. Hancock,[‡] and Suzana K. Straus[†*]
[†]Department of Chemistry and [‡]Centre for Microbial Diseases and Immunity Research, University of British Columbia, Vancouver, British Columbia, Canada

ABSTRACT The effects of hydrophobic thickness and the molar phosphatidylglycerol (PG) content of lipid bilayers on the structure and membrane interaction of three cationic antimicrobial peptides were examined: aurein 2.2, aurein 2.3 (almost identical to aurein 2.2, except for a point mutation at residue 13), and a carboxy C-terminal analog of aurein 2.3. Circular dichroism results indicated that all three peptides adopt an α-helical structure in the presence of a 3:1 molar mixture of 1,2-dimyristoyl-*sn*-glycero-3-phosphocholine/1,2-dimyristoyl-*sn*-glycero-3-[phospho-*rac*-(1-glycerol)] (DMPC/DMPG), and 1:1 and 3:1 molar mixtures of 1-palmitoyl-2-oleoyl-*sn*-glycero-3-phosphocholine/1-palmitoyl-2-oleoyl-*sn*-glycero-3-[phospho-*rac*-(1-glycerol)] (POPC/POPG). Oriented circular dichroism data for three different lipid compositions showed that all three peptides were surface-adsorbed at low peptide concentrations, but were inserted into the membrane at higher peptide concentrations. The ^{31}P solid-state NMR data of the three peptides in the DMPC/DMPG and POPC/POPG bilayers showed that all three peptides significantly perturbed lipid headgroups, in a peptide or lipid composition-dependent manner. Differential scanning calorimetry results demonstrated that both amidated aurein peptides perturbed the overall phase structure of DMPC/DMPG bilayers, but perturbed the POPC/POPG chains less. The nature of the perturbation of DMPC/DMPG bilayers was most likely micellization, and for the POPC/POPG bilayers, distorted toroidal pores or localized membrane aggregate formation. Calcein release assay results showed that aurein peptide-induced membrane leakage was more severe in DMPC/DMPG liposomes than in POPC/POPG liposomes, and that aurein 2.2 induced higher calcein release than aurein 2.3 and aurein 2.3-COOH from 1:1 and 3:1 POPC/POPG liposomes. Finally, DiSC$_3$5 assay data further delineated aurein 2.2 from the others by showing that it perturbed the lipid membranes of intact *S. aureus* C622 most efficiently, whereas aurein 2.3 had the same efficiency as gramicidin S, and aurein 2.3-COOH was the least efficient. Taken together, these data show that the membrane interactions of aurein peptides are affected by the hydrophobic thickness of the lipid bilayers and the PG content.

INTRODUCTION

Cationic antimicrobial peptides are an important class of compounds that are being explored as alternatives to currently used antibiotics, because of their unique property of displaying few to no resistance effects (1–3). They are ubiquitous in nature, and constitute an important part of the immune defense system of many plants and animals. For example, amphibians secrete a range of cationic antimicrobial peptides as part of their host-defense mechanism (4,5). A number of these were studied extensively, and include magainins (6–15), maculatins (16–21), brevinins (22–27), and others, such as citropin 1.1 and aurein 1.2 from the Australian tree frogs *Litoria citropa* and *Litoria aurea* (16–19,21,28–30), respectively. The latter peptide is part of a larger family of peptides known as aurein peptides, which range in length from 13–25 residues. Many aurein peptides possess an amidated C-terminus and exhibit broad-spectrum antimicrobial activity against Gram-positive bacteria such as *Bacillus cereus*, *Leuconostoc lactis*, *S. aureus*, and *S. epidermis*, as well as other disease-causing agents, such as cancerous cells (29).

Aurein 1.2 is by far the most studied member of the aurein peptide family. It is a 13-residue peptide, with a net positive charge of +1. Solution-state NMR and circular-dichroism studies showed that it adopts an α-helical conformation in membrane mimetic environments (30,31). Because the length of aurein 1.2 is too short (~19.5 Å) (16) to span fluid lipid bilayers, it was proposed that this peptide interacts primarily with the membrane interface, and promotes bilayer damage by a detergent-like or carpet-like mechanism. Recently, aurein 1.2 was shown to be an effective bactericidal agent against staphylococci and streptococci (32). Moreover, it was found to have relatively low cytotoxicity, and to act in synergy with other antibiotics such as minocycline or clarithromycin. Because these antibiotics are hydrophobic, it is believed that the membrane perturbation induced by aurein 1.2 facilitates the entry of minocycline or clarithromycin into the membrane, making them more effective (33,34). The ability of aurein 1.2 to perturb membranes was recently examined in detail, using differential scanning calorimetry and Fourier transform infrared spectroscopic studies (35).

In our previous work, we examined two other members of the aurein peptide family, i.e., aurein 2.2 (GLFDIVKKVVG A**L**GSL-CO**NH$_2$**) and aurein 2.3 (GLFDIVKKVVGA**I**GS L-CO**NH$_2$**), as well as an inactive version of aurein 2.3 with an anionic carboxy C-terminus (aurein 2.3-COOH). Each of these peptides is 16 residues in length, with a net

Submitted July 15, 2008, and accepted for publication October 9, 2008.

*Correspondence: sstraus@chem.ubc.ca

Editor: Huey W. Huang.

0006-3495/09/01/0552/14 $2.00

doi: 10.1016/j.bpj.2008.10.012

charge of +2 for the amidated versions at neutral pH. Using solution-state circular dichroism and ^{1}H NMR spectroscopy, it was demonstrated that the three aurein peptides adopt a continuous α-helical structure in the presence of trifluoroethanol (TFE), 1,2-dimyristoyl-*sn*-glycero-3-phosphocholine (DMPC), and 1:1 DMPC/1,2-dimyristoyl-*sn*-glycero-3-[phospho-*rac*-(1-glycerol)] (DMPG) (mol/mol) small unilamellar vesicles (SUVs) (36). Further model membrane studies, using oriented circular dichroism spectroscopy (OCD), showed that aurein 2.2 and aurein 2.3 effectively perturb the 1:1 DMPC/DMPG (mol/mol) bilayers (bacterium-like membranes), while displaying minor effects on DMPC bilayers (mammalian-like membranes) (36). In contrast, aurein 2.3-COOH showed a decreased ability to insert into DMPC/DMPG bilayers, but a slightly greater ability to perturb DMPC bilayers (36).

To determine the mode of action of cationic antimicrobial peptides in general, it is important to establish the nature of the interaction of peptides with model membrane bilayers. Over the years, a number of lipids have been used for such studies: 1-palmitoyl-2-oleoyl-*sn*-glycero-3-phosphocholine (POPC) (e.g., MSI-78 and MSI-594) (37), 1,2-dimyristoyl-*sn*-glycero-3-phosphocholine (DMPC) (e.g., aurein 1.2) (19), 1,2-diphytanoyl-*sn*-glycero-3-phosphatidylcholine (DPhPC) (e.g., alamethicin) (38,39), and other diacylphosphatidylcholine membranes (e.g., $K_2(LA)_xK_2$) (40), or lipid mixtures, such as POPC/1-palmitoyl-2-oleoyl-*sn*-glycero-3-[phospho-*rac*-(1-glycerol)] (POPG) (e.g., MSI-78 and MSI-594) (37) and DMPC/DMPG (e.g., PGLa) (41), to name but a few. To describe peptide-lipid interactions completely, a range of parameters such as peptide/lipid ratio, membrane composition, temperature, hydration, buffer composition (42), and lipid phase (39) must be taken into account. Most importantly, the results from such studies must be correlated with assays performed on live bacteria, e.g., the $DiSC_35$ assay that assesses the depolarization of cytoplasmic membranes, to determine biological relevance.

To elucidate a more comprehensive mechanism of action for aurein 2.2 and aurein 2.3, we examined the effect of lipid bilayer thickness and molar phosphatidylglycerol (PG) content on the ability of peptides to perturb membranes, using the most widely used lipid mixtures, i.e., 1:1 and 3:1 mixtures of DMPC/DMPG and POPC/POPG. Given that the two peptides differ in sequence only at position 13, we wanted to establish whether the modest change in going from leucine to isoleucine had any effect on peptide-lipid interactions. This was of particular interest because the original reports indicated that aurein 2.2 was four times more active than aurein 2.3, as determined by minimal inhibitory concentrations (MICs) (30). Although in our hands the MICs for these two peptides were closer to one another (36), and although it is well-known that some variability exists in the determination of MICs (e.g., variations by factors of 2), it is still important to understand what effect the amino acid sequence (e.g., hydrophobicity or electrostatics) exerts on structure and membrane interaction, and how that, in turn, affects antimicrobial activity (43–47). As in our previous study, we used aurein 2.3-COOH, an inactive version of aurein 2.3, as a benchmark.

Here, we used solution circular dichroism (CD) spectroscopy to determine whether any structural changes of the three aurein peptides occurred in different lipid vesicles. To assess how activity may be influenced by different membrane composition, we determined the interaction between three aurein peptides and various lipid bilayers, using OCD, ^{31}P NMR spectroscopy, and differential scanning calorimetry (DSC). We conducted calcein release assays (using DMPC/DMPG and POPC/POPG model membranes) and 3,3′-dipropylthiadicarbocyanine iodide ($DiSC_35$) assays (using *S. aureus* C622) to examine whether leakage is sequence-dependent or lipid composition-dependent. Overall, these data should allow us to determine the best bacterial model membranes to study this family of cationic antimicrobial peptides, and to understand better how sequence modulates function.

MATERIALS AND METHODS

Materials

Fmoc-protected amino acids, Wang and Rink resin, and 2-(1H-benzotriazol-1-yl)-1,1,3,3-tetramethyluronium hexafluorophosphate (HBTU) were purchased from Advanced ChemTech (Louisville, KY). We obtained *N*-hydroxybenzotiazhole (HOBt) from Novabiochem (San Diego, CA). We purchased *N*,*N*-dimethylformamide (DMF), dichloromethane (DCM), acetonitrile (AcN), and potassium nitrate from Fisher Chemicals (Nepean, Ontario, Canada). The *N*,*N*-diiopropylethylamine (DIEA), trifluoroacetic acid (TFA), ethane dithiol (EDT), and triethylsilane (TES) were obtained from Sigma-Aldrich (St. Louis, MO). Mylar plates were made by cutting Melinex Teijin films from Dupont (Wilton, United Kingdom). The 1,2-dimyristoyl-*sn*-glycero-3- phosphocholine (DMPC), 1,2-dimyristoyl-*sn*-glycero-3-[phospho-*rac*-(1-glycerol)] (DMPG), 1-palmitoyl-2-oleoyl-*sn*-glycero-3-phosphocholine (POPC), and 1-palmitoyl-2-oleoyl-*sn*-glycero-3-[phospho-*rac*-(1-glycerol)] (POPG) were purchased from Avanti Polar Lipids (Alabaster, AL), and were obtained dissolved in chloroform. We purchased bis[*N*,*N*–bis(carboxymethyl)aminomethyl]fluorescein (calcein) and 3,3′- $DiSC_35$ from Sigma-Aldrich.

Peptide synthesis

Aurein 2.2, aurein 2.3, and aurein 2.3-COOH were synthesized as previously described (36), using a peptide synthesizer from CS Bio Co. (Menlo Park, CA) and in situ neutralization Fmoc chemistry, with Rink or Wang resin, as appropriate. The C-terminal Leu was double-coupled (i.e., allowed to couple to the resin for 60 min, washed, and allowed to couple to resin for a further 60 min before the next step in the peptide synthesis), to improve the yield.

Purification

The crude peptide product was purified by preparative reverse phase high-performance liquid chromatography on a Waters (Mississauga, Ontario, Canada) 600 system with 229-nm ultraviolet detection, using a Phenomenex (Torrance, CA) C4 preparative column (20.0 μm, 2.1 cm × 25.0 cm), as previously described (36). The identity of products was verified using

electrospray ionization mass spectrometry and MALDI-TOF, as previously described (36), and confirmed to be ~98–99% pure.

Solution CD sample preparation

Solution CD samples with a constant peptide concentration of 2.0 mM were prepared in different peptide/lipid (P/L, either DMPC/DMPG or POPC/POPG) molar ratios of 1:15, 1:50, and 1:100 (or 6.7, 2.0, and 1.0 mol % of peptide with respect to lipids). Appropriate amounts of lipids in chloroform were dried, using a stream of air to remove most of the chloroform, and vacuum-dried overnight in a 5.0-mL round-bottom flask. After adding 500 μL of ddH_2O and 0.1 μmol (0.16 mg) of peptide to dried lipids, the mixture was sonicated in a water bath for a minimum of 30 min (until the solution was no longer turbid), to ensure lipid vesicle formation. For all samples, corresponding background samples without peptides were prepared for spectral subtraction.

Mechanically oriented sample preparation

Solid-state NMR samples were prepared for three different P/L molar ratios: 1:15, 1:80, and 1:120, following procedures similar to those reported (48,49). The amount of lipids (dissolved in chloroform) was kept constant at 9.59 μmol. The lipid was dried using a stream of air to remove most of the chloroform, and vacuum-dried overnight in a 5-mL round-bottom flask. Then the appropriate amount of peptide was added, and the mixture was redissolved in 400 μL of ddH_2O by sonication. The mixture was deposited in 10-μL portions repeatedly onto nine Mylar plates placed in a petri dish. Between depositions, most of the ddH_2O was evaporated before the next portion was deposited onto the plate. The plated samples were then placed in a 93% relative humidity chamber, and were indirectly hydrated by incubating inside a dessicator at 37°C for 5 days (DMPC/DMPG) or 7 days (POPC/POPG). The humidity of samples was verified by visual inspection (well-hydrated samples are translucent). The degree of alignment was verified by ^{31}P solid-state NMR. Consistent sample preparation was verified by preparing 2–3 samples for each lipid composition and peptide concentration. Finally, plated samples were wrapped in a thin layer of parafilm, and placed in plastic sheathing before data acquisition.

Oriented CD samples were prepared in a similar fashion to that described above. The peptide amount was kept constant at 0.5 μmol (0.81 mg), and mixed with appropriate molar ratios of lipids, i.e., 1:15, 1:30, 1:40, 1:80, and 1:120 P/L ratios (or 6.67, 3.33, 2.50, 1.25, and 0.83 mol % of peptide with respect to lipids), and sonicated in 2 mL of ddH_2O. Each mixture was deposited in 90-μL portions onto 3 cm × 1 cm and 1-mm-thick quartz slides, cleaned thoroughly with ddH_2O and ethanol before sample preparation. Clear layers of samples were evident on the slides after indirect hydration of the samples. Before CD spectral acquisition, each sample was covered with a second slide with a spacer (six layers of stacked parafilm, in a rectangular 3 cm × 1 cm frame with a 2-mm width) in between.

Circular dichroism

Solution and oriented CD experiments were performed using a J-810 spectropolarimeter (Jasco, Victoria, British Columbia, Canada) at 30°C, as previously described (36). Briefly, spectra were obtained over a wavelength range of 185–250 nm, using continuous scanning mode with a response of 1 s with 0.5-nm steps, a bandwidth of 1.5 nm, and a scan speed of 20 nm/min. The signal/noise ratio was increased by acquiring each spectrum over an average of three scans. Finally, each spectrum was corrected by subtracting the background from the sample spectrum. The temperature was kept constant by means of a water bath.

NMR spectroscopy

Solid-state ^{31}P NMR experiments on mechanically aligned lipid bilayer samples were performed on a 500-MHz NMR spectrometer (Bruker Biospin, Milton, Ontario, Canada) at 30°C, operating at a phosphorus frequency of 202.48 MHz, as previously reported (36). The 90° pulse was set to 12.5 μs (DMPC/DMPG) or 10.5 μs (POPC/POPG), and a 3-s recycle delay was used. Spectra were acquired using 2048 scans, and were processed without any line-broadening.

Calcein release assays

Appropriate amounts of lipids for a specific lipid mixture were weighed and dissolved in chloroform (1–2 mL) in a glass vial. Chloroform was then evaporated under a stream of nitrogen, and the lipid mixture was further dried under vacuum for at least 2 h. Calcein resuspending buffer was prepared by dissolving 62 mg of calcein in 1 mL of 5.0 mM HEPES buffer, pH 7.5 (final concentration, 100 mM). The NaOH was added in small aliquots until calcein dissolved, to yield a dark orange solution. Calcein release buffer was then added to the lipid mixture, which underwent five cycles of freezing and thawing. Liposomes were extruded through two double-stacked 0.1-μm membranes. The extruded calcein-entrapped liposomes were then separated from free calcein in solution, using a Sephadex G50 column (GE Healthcare, Piscataway, NJ) which was rehydrated overnight in 20 mM HEPES, 150 mM NaCl, and 1.0 mM EDTA, pH 7.4. The rehydrating buffer was also used as the eluting buffer.

Calcein-free liposomes were prepared using the same procedure, but without using calcein in the resuspending buffer. We prepared 1.5 mL of the calcein-free liposomes because of their greater usage during the assay. The lipid mixture was resuspended in 20 mM HEPES, 150 mM NaCl, and 1.0 mM EDTA, pH 7.4, and extruded as above, without running through the Sephadex G50 column.

The calcein release assay was performed by combining 2 mL of 20 mM HEPES, 150 mM NaCl, 1.0 mM EDTA (pH 7.4), 3.75 μL of calcein-entrapped liposomes, and 7.5 μL of calcein-free liposomes in a cuvette, with slow stirring. Fluorescence was measured using a 640-10S spectrofluorimeter (PerkinElmer, Waltham, MA), with an excitation wavelength of 490 nm and an emission wavelength of 520 nm. A slit width of 6 nm was generally used, but could be adjusted to achieve maximum fluorescence. Baseline fluorescence was established for ~100 s. Maximum fluorescence was determined by adding 0.1% Triton X-100 as a control. After establishing baseline and maximum fluorescence, the peptides of interest were added to perform the assay. Gramicidin S was used as a positive control.

DiSC$_3$5 assays

The ability of aurein peptides to depolarize the cytoplasmic membrane of *S. aureus* C622 was determined, using the membrane potential sensitive dye DiSC$_3$5. The C622 was grown to mid-logarithmic phase in Luria Broth medium, centrifuged, washed in 5 mM HEPES and 20 mM glucose, and resuspended in the same buffer to a final OD_{600} of 0.05. A final concentration of 200 mM KCl was added to the cells and left for 30 min at room temperature, to equilibrate cytoplasmic and external K^+ concentrations, before DiSC$_3$5 was added at a final concentration of 0.8 μM for 30 min.

Changes in fluorescence resulting from disruption of the membrane potential were measured up to 5 min, using a 640-10S spectrofluorimeter (PerkinElmer), with an excitation wavelength of 622 nm and an emission wavelength of 670 nM after the addition of each aurein peptide at 1 ×, 2 ×, and 5 × MIC (as previously ascertained) (36) to 2-mL cell suspension in a 1-cm quartz cuvette. Aurein 2.3-COOH was only tested at 1 × MIC because of its high MIC. All membrane permeabilization results were compared to gramicidin S, used as a positive control.

Differential scanning calorimetry

Each aurein peptide was added at a 1:15 aurein/lipid molar ratio to multilamellar vesicles of 1:1 DMPC/DMPG or 1:1 POPC/POPG (25 mg/mL) resuspended in HEPES buffer (20 mM HEPES, pH 7.0, 100 mM

NaCl). Samples were degassed for 5 min before loading the sample into a VP-DSC or multicell DSC (Calorimetry Sciences, South Provo, UT), located at the University of British Columbia Centre for Biological Calorimetry. Samples were heated and cooled over a temperature range of 1–70°C at a rate of 1.00°C/min (DMPC/DMPG), or −20–70°C at a rate of 0.33°C/min (POPC/POPG). The resulting data were converted to units of molar heat capacity, after baseline correction by subtracting a blank buffer scan.

RESULTS

Secondary structure of aurein peptides by solution CD spectroscopy

Our previous studies showed that the aurein 2.2, aurein 2.3, and aurein 2.3-COOH peptides adopt an α-helical structure in the presence of TFE, DMPC, and 1:1 DMPC/DMPG (mol/mol) SUVs (36). To verify that these peptides remain structured in the different lipid environments probed here, solution CD experiments were performed, using different lipid mixtures and P/L ratios.

Fig. 1 shows the solution CD results of the three aurein peptides in 1:1 POPC/POPG SUVs. Additional solution CD results of the three aurein peptides in 3:1 DMPC/DMPG and 3:1 POPC/POPG SUVs are included in the Supporting Material (Fig. S1). All spectra consisted predominantly of a maximum at 190 nm and two minima at 210 nm and 222 nm, which are characteristic of α-helical structure. All spectra were fitted using three different programs, CDSSTR (50), CONTINLL (51), and SELCON3 (52–54), using either the full data set or half the data set (using only points at every 1 nm in a range of 190–260 nm) to estimate error (Table S1). The results demonstrate that all three aurein peptides adopt close to 100% α-helical conformation at high P/L ratios (as also found in 50% TFE/H_2O; Table S1). As reported previously (36), similar intensities were evident for all P/L molar ratios studied (P/L = 1:15, 1:50, and 1:100) for 3:1 DMPC/DMPG, indicating that maximum binding of the peptide to lipid vesicles occurred. Saturation would be observed with a combination of signals from both α-helical and random-coil structures (19). For POPC/POPG (1:1 or 3:1), on the other hand, the helical content increased with increased peptide concentrations, indicating that high concentrations are needed to achieve maximum binding. Overall, the data show that the three aurein peptides were dependent on the molar concentrations or types of phospholipids examined.

Membrane insertion states of aurein peptides, using OCD spectroscopy

Understanding the interactions of aurein peptides with different model membranes is crucial in elucidating the effects of membrane composition on the extent of peptide insertion into lipid bilayers. We performed OCD experiments to investigate the peptide insertion profiles in different lipid bilayers. For both OCD and ^{31}P solid-state NMR, samples

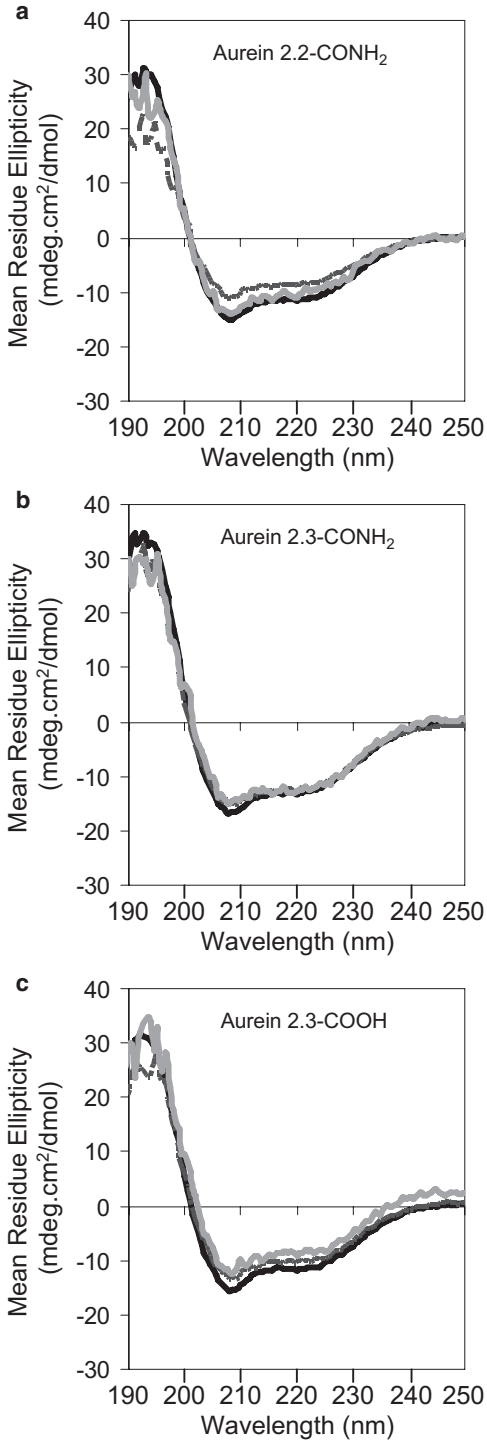

FIGURE 1 Solution CD spectra of aurein peptides in 1:1 POPC/POPG (mol/mol) SUVs: (*a*) aurein 2.2; (*b*) aurein 2.3; and (*c*) aurein 2.3-COOH (*solid black line*, P/L = 1:15; *dotted line*, P/L = 1:50; *solid gray line*, P/L = 1:100). Spectra indicate that aurein peptides adopt an α-helical conformation in the presence of POPC/POPG SUVs. Data for additional lipid compositions can be found in the Supporting Material. The percentage of α-helical content is reported in Table S1.

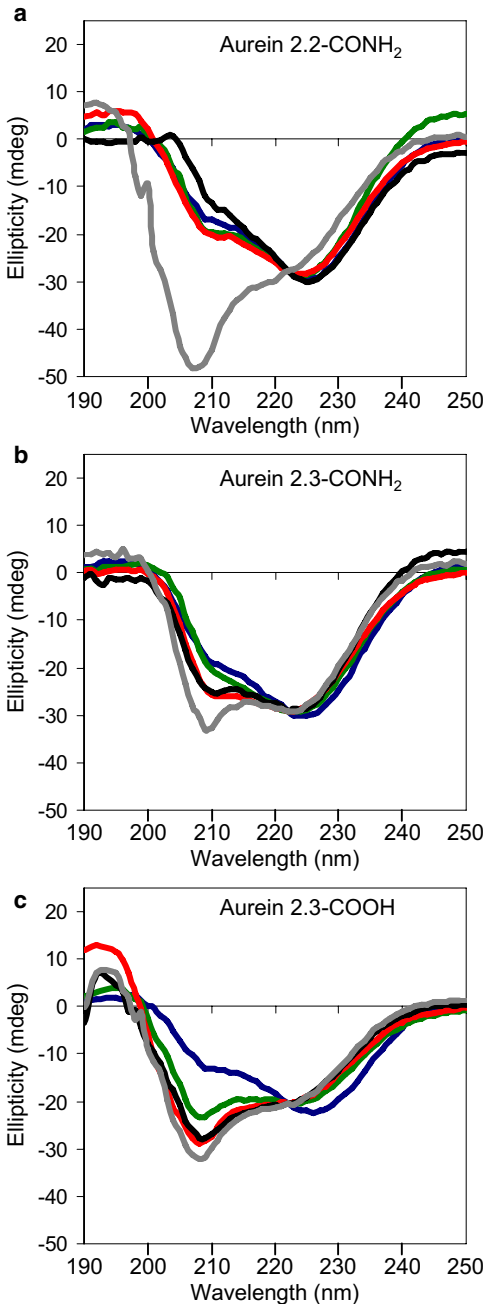

FIGURE 2 Oriented CD spectra of aurein peptides in 1:1 POPC/POPG (mol/mol) bilayers: (*a*) aurein 2.2; (*b*) aurein 2.3; and (*c*) aurein 2.3-COOH. P/L molar ratios = 1:15 (*blue*), 1:30 (*green*), 1:40 (*red*), 1:80 (*black*), and 1:120 (*gray*). Spectra were normalized such that intensities of all spectra at 222 nm are the same. The spectra show that peptides insert into 1:1 POPC/POPG (mol/mol) bilayers at threshold P/L molar ratios between 1:80 and 1:120 for aurein 2.2, between 1:40 and 1:30 for aurein 2.3, and between 1:15 and 1:30 for aurein 2.3-COOH. Data for additional lipid compositions can be found in the Supporting Material.

were prepared in a similar fashion, so that the data sets could be compared directly, and so that we could verify that samples were aligned. All experiments were conducted at 30°C (liquid crystalline phase), for consistent comparisons with our previous study. In addition, experiments were repeated at least twice, to ensure reproducibility of the results.

Fig. 2 shows OCD results for the aurein peptides in 3:1 DMPC/DMPG, 1:1 POPC/POPG, and 3:1 POPC/POPG (mol/mol) bilayers as a function of P/L ratio. Spectra were scaled so that the minimum at 222 nm had the same intensity. The spectra in Fig. S2, *a–c*, showed that the three aurein peptides inserted (inserted, I-state; or tilt, T-state) into a 3:1 DMPC/DMPG bilayer at threshold P/L molar ratios between 1:40 and 1:80, and became surface-adsorbed (S-state) at P/L ratios >1:80 (mol/mol). This is in contrast to previously reported OCD data in 1:1 DMPC/DMPG (mol/mol) bilayers (36), where all three peptides were already in the I-state or T-state at P/L ratios of 1:120. For 1:1 POPC/POPG (mol/mol) bilayers (Fig. 2, *a–c*, or Fig. S2, *d–f*), each peptide inserted differently: the threshold P/L molar ratio was between 1:80 and 1:120 for aurein 2.2, between 1:40 and 1:30 for aurein 2.3, and between 1:15 and 1:30 for aurein 2.3-COOH. Finally, the spectra in Fig. S2, *g–i*, show that the three aurein peptides inserted into the 3:1 POPC/POPG bilayer at threshold P/L molar ratios between 1:40 and 1:80.

The data illustrate that both molar PG content and bilayer thickness played a role in peptide insertion profiles. A decrease in molar PG content and an increase in bilayer thickness progressively reduced the insertion ability of the amidated peptides. High molar PG content and increased bilayer thickness resulted in an inability of aurein 2.3-COOH to insert into 1:1 POPC/POPG bilayers, except at high peptide concentrations. Because the DMPC/DMPG and POPC/POPG bilayer hydrophobic thickness are ~26.5 Å (55,56) and ~39 Å (57) in the liquid crystalline phase, respectively, the three aurein peptides would not have sufficient peptide length (hydrophobic length, ~24 Å) to span the lipid bilayer entirely, particularly in the long-chained POPC/POPG bilayers. Unfavorable electrostatic interactions between the negatively charged C-terminus and the negatively charged PG headgroups probably explain the high aurein 2.3-COOH peptide concentrations needed to permit insertion into the lipid bilayers at increased molar PG content (43).

Lipid headgroup perturbation by aurein peptides with ^{31}P solid-state NMR spectroscopy

We recorded ^{31}P NMR spectra for all peptides in 4:1 DMPC/DMPG (mol/mol) (Fig. 3) and 4:1 POPC/POPG (mol/mol) (Fig. 4) bilayers. These lipid compositions were chosen because in both cases, all three peptides show similar concentration-dependent insertion profiles (as in the 3:1 cases presented above). The ^{31}P NMR experiments were conducted to determine whether the insertion of peptides was accompanied by a perturbation of the lipid headgroups, and whether this membrane disruption occurred via a barrel-stave, carpet, or toroidal pore (15,58–61), a micellar

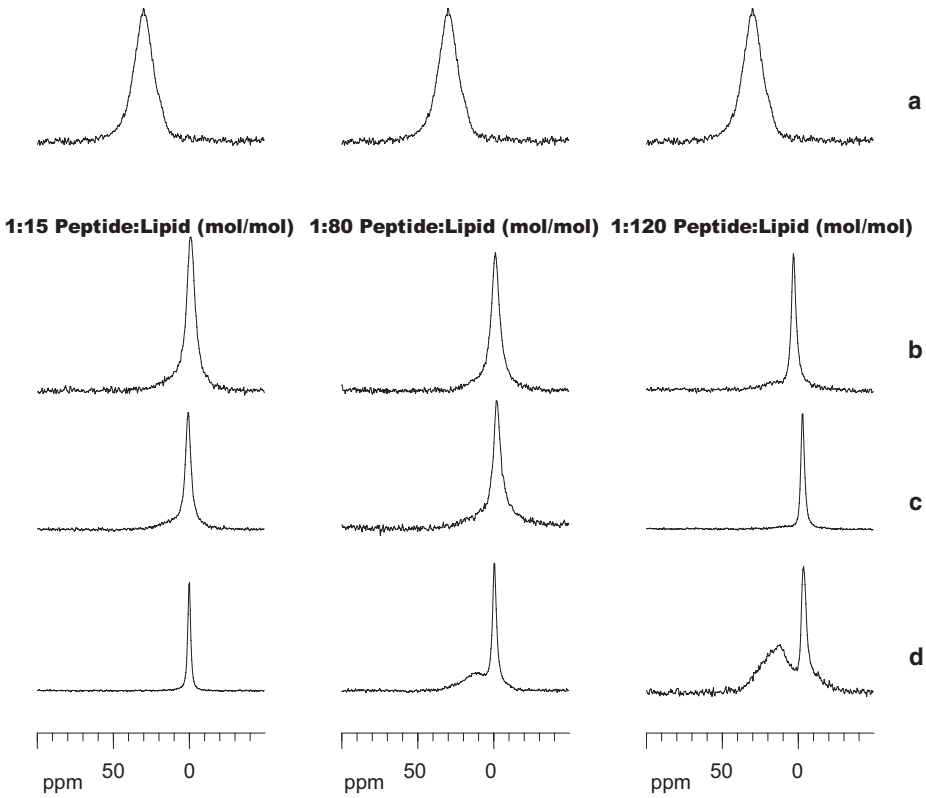

FIGURE 3 Solid-state ^{31}P NMR spectra of mechanically aligned 4:1 DMPC/DMPG (mol/mol) bilayers containing three aurein peptides: (*a*) DMPC/DMPG bilayers alone, or (*b*) aurein 2.2, (*c*) aurein 2.3, and (*d*) aurein 2.3-COOH. For the 1:15 P/L ratio, we used 1.03 mg of peptide. For the 1:80 P/L ratio, we used 0.19mg of peptide. For the 1:120 P/L ratio, we used 0.13 mg of peptide. Spectra were recorded using 2048 scans at 30°C, oriented such that the bilayer normal was parallel to the external magnetic field. Spectra were processed without any line-broadening.

aggregate channel (62,63), or a detergent-like mechanism (42).

In Fig. 3 *a*, in the absence of aurein peptides, a single ^{31}P spectral peak was observed at ~30 ppm. This finding illustrates that the phosphorus headgroups of 4:1 DMPC/DMPG (mol/mol) bilayers were well-aligned, with the bilayer normal parallel to the magnetic field. The presence of peptides significantly changed the physical state of DMPC/DMPG bilayers (Fig. 3, *b–d*). The peak at 30 ppm disappeared when the amidated peptides were added to the DMPC/DMPG bilayers, and a new, sharp, narrow peak (with small powder-pattern signals) appeared, and shifted to 0 ppm. This indicates that the phosphorus headgroups of 4:1 DMPC/DMPG (mol/mol) mixtures were highly curved in the presence of aurein 2.2 and aurein 2.3. Indeed, a number of other solid-state NMR studies of antimicrobial peptides (12,64–66) demonstrated that the presence of a peak at 0 ppm is indicative of either small lipid vesicle/micelle formation or a different lipid-phase formation. When aurein 2.3-COOH was added at high concentrations, the spectrum displayed a similar single, narrow, upfield-shifted peak (Fig. 3 *d*). However, at low concentrations of aurein 2.3-COOH, the peak at 30 ppm did not disappear completely. This finding suggests that partial alignment was still maintained, and complete destabilization of the lipid bilayers did not occur. The orientation of bilayer headgroups was not affected as significantly by aurein 2.3-COOH at low P/L molar ratios. This finding was consistent with our current (Fig. S2) and previous (36) OCD results, i.e., that aurein 2.3-COOH does not insert readily into the DMPC/DMPG bilayers at a 1:120 P/L molar ratio.

In contrast to DMPC/DMPG bilayers, the aurein peptides affected the thicker 4:1 POPC/POPG (mol/mol) bilayers differently (Fig. 4). In the absence of peptides, spectra consisted primarily of a single resonance at 30 ppm, which again indicated that the lipid bilayers were aligned with their normal parallel to the magnetic field (Fig. 4 *a*). The minor peak at −10 ppm represented the signal from a small percentage of unaligned bilayer headgroups, as observed in other studies (65,66). In the presence of amidated aurein peptides, the spectra showed an increased contribution from unaligned ^{31}P headgroups and a broadened peak at 30 ppm. In addition, a powder-pattern signal was also observed at −10 to 30 ppm, indicative of random headgroup orientations (Fig. 4, *b* and *c*). These changes in the spectra occurred for all P/L molar ratios and both aurein 2.2 and aurein 2.3, suggesting no obvious dependence on peptide sequence and concentration. When aurein 2.3-COOH was added at high concentrations, the spectrum seemed similar to its amidated counterparts. At low peptide concentrations, however, the two individual peaks at −10 ppm and 30 ppm disappeared, and broadened powder-pattern signals were evident. This finding may indicate that aurein 2.3-COOH perturbed the phosphorus headgroups in a way slightly different from that of amidated peptides at low peptide concentrations (Fig. 4 *d*). The

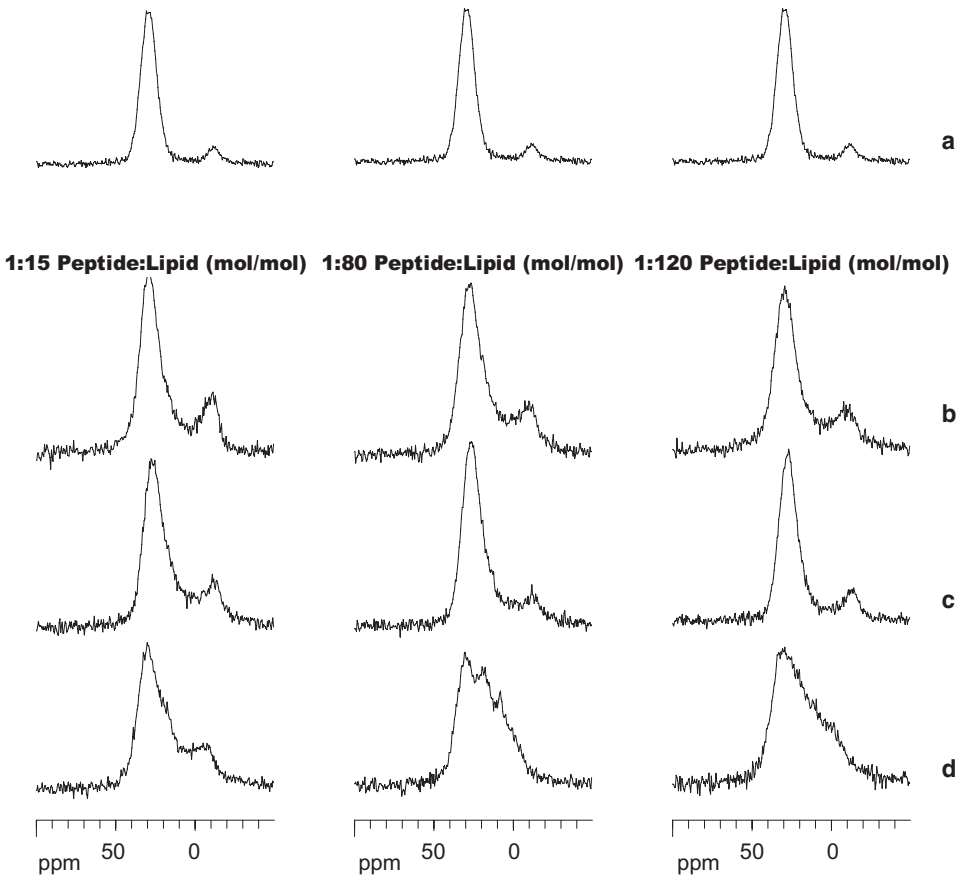

FIGURE 4 Solid-state ^{31}P NMR spectra of mechanically aligned 4:1 POPC/POPG (mol/mol) bilayers containing three aurein peptides: (*a*) POPC/POPG bilayers alone, or containing (*b*) aurein 2.2, (*c*) aurein 2.3, and (*d*) aurein 2.3-COOH. For the 1:15 P/L ratio, we used 1.03 mg of peptide. For the 1:80 P/L ratio, we used 0.19 mg of peptide. For the 1:120 P/L ratio, we used 0.13 mg of peptide. Spectra were recorded using 2048 scans at 30°C, oriented such that the normal bilayer was parallel to the external magnetic field. Spectra were processed without any line-broadening.

underlying powder pattern indicates that aurein peptides may disorder the bilayer headgroups by formation of a toroidal pore (15,58–61). The extent of membrane perturbation was not found to be concentration-dependent or peptide-specific (at least for the amidated versions).

Lipid-chain perturbation by aurein peptides, using DSC

Observations of phase-transition changes provide information on the overall phase structural integrity of lipid membranes in the presence of antimicrobial peptides. We performed DSC experiments to determine whether aurein 2.2 and aurein 2.3 affected the lipid chains, and we observed how these peptides disrupted the phase structure of lipid membranes.

Fig. 5 *a* shows DSC thermograms of 1:1 DMPC/DMPG (mol/mol) liposomes in the absence and presence of aurein 2.2, aurein 2.3, and aurein 2.3-COOH (P/L, 1:15). In the absence of peptides, the thermogram consisted of a pretransition peak at 17.5°C and a main phase transition peak at 24.5°C, consistent with findings in the literature (67). In the presence of amidated peptides, the pretransition peak remained similar, whereas the main-phase transition peak broadened and was almost completely abolished. This finding indicated that both aurein 2.2 and aurein 2.3 disrupted lipid membranes severely, such that only a small lamellar-liquid crystalline coexistence regime remained. For aurein 2.3-COOH, the main transition peak was severely broadened as well, but not to the extent of the amidated peptides. The broadened main-phase transition peak was also an indication of membrane curvature in the presence of peptides, consistent with the ^{31}P NMR data presented above for 4:1 DMPC/DMPG. A similar pretransition peak for the amidated peptides indicates that the low-temperature phase domains remained intact, suggesting that these peptides did not affect the low-temperature phase domains significantly.

Fig. 5 *b* shows a thermogram of 1:1 POPC/POPG (mol/mol) in the absence and presence of aurein 2.2, aurein 2.3, and aurein 2.3-COOH (P/L, 1:15). In the absence of peptides, the thermogram exhibited a single main-phase transition peak at −2°C. In the presence of aurein 2.2, the transition peak shifted to a slightly higher temperature (−1°C). In the presence of aurein 2.3, however, the transition temperature did not change significantly. Finally, in the presence of aurein 2.3-COOH, the transition temperature was −3°C. For all peptides, the transition peak intensity was slightly different when the peptides were present. This finding indicates that both amidated aurein peptides did not have

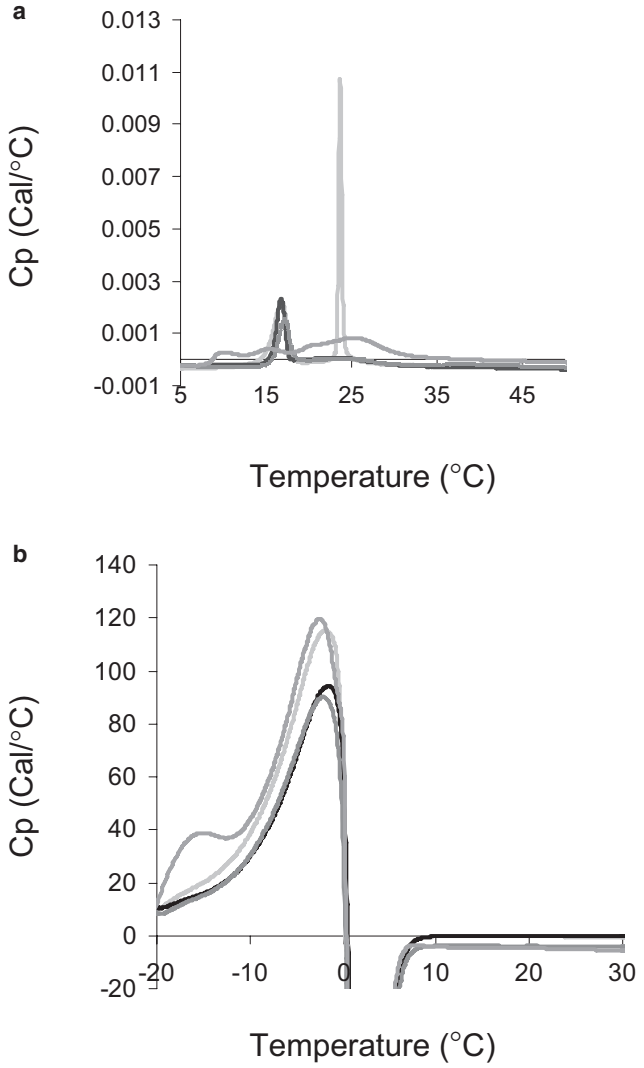

FIGURE 5 DSC thermograms of (*a*) 1:1 DMPC/DMPG (mol/mol) and (*b*) 1:1 POPC/POPG (mol/mol) liposomes in the absence (*light gray solid line*) and presence of aurein 2.2 (*black solid state*), aurein 2.3 (*dark gray solid line*), and aurein 2.3-COOH (*gray*) at a 1:15 P/L molar ratio.

pronounced effects on the chain-melting event, and most likely perturbed the headgroups more than the acyl chains. Together with the ^{31}P NMR data, these findings indicate that aurein peptides most likely induce toroidal pore formation (i.e., either a distorted toroidal or localized membrane aggregate model) in POPC/POPG bilayers.

Membrane leakage induced by aurein peptides in model membranes, as determined in calcein release assays

Given the results above, calcein release assays were used to further determine to what extent the aurein peptides cause membrane disruption. In general, the assay probes the increase in fluorescence when the fluorophore (calcein) is released as a result of membrane leakage. Gramicidin S, a cyclic antimicrobial peptide, acted as positive control in these assays. The units of fluorescence were arbitrary, and set to a range of 0–1000. The assay was performed for a minimum of 300 s.

Table 1 summarizes relative percentages of aurein peptide-induced calcein release with reference to the positive control 0.1% Triton-X (set to 100%) at different P/L molar ratios in different membranes. The three aurein peptides caused significant calcein release at 1:15 P/L molar ratios, and only minimal ($\leq$6%) release at lower concentrations. All three aurein peptides caused nearly 100% calcein release from 3:1 DMPC/DMPG liposomes at high peptide concentrations. In POPC/POPG liposomes, on the other hand, the aurein peptides were less effective at causing membrane leakage. Indeed, at a 1:15 P/L molar ratio, aurein 2.2 induced the highest calcein release (27% and 36% in 1:1 and 3:1 POPC/POPG, respectively), whereas aurein 2.3 caused a slightly lower calcein release than did aurein 2.3-COOH from POPC/POPG liposomes (Table 1). It is noteworthy that in 3:1 POPC/POPG, aurein 2.2 is a factor of 2–3 times more effective at perturbing liposomes that aurein 2.3 and aurein 2.3-COOH, which are equally effective. This finding suggests that changing the nature of the C-terminus has little effect on the capacity of these peptides to perturb model membranes. At 1:80 and 1:120 P/L ratios, all aurein peptides did not significantly disrupt 1:1 and 3:1 POPC/POPG liposomes, consistent with our OCD results.

Fig. 6 *a* shows the calcein release assay results of aurein peptides in 3:1 DMPC/DMPG (*top*), 1:1 (*middle*), and 3:1 POPC/POPG (*bottom*) (mol/mol) liposomes at 1:15 P/L molar ratio. No obvious difference in the percentage of calcein released was evident, compared with 3:1 DMPC/DMPG (mol/mol) membranes in the presence of the peptides. When added to 1:1 and 3:1 POPC/POPG (mol/mol) membranes, aurein 2.2 induced higher calcein release than did the two aurein 2.3-related peptides. Surprisingly, aurein 2.3-COOH induces more leakage that aurein 2.3 at steady state (t >200s), although aurein 2.3 perturbs membranes better

TABLE 1 Percentage of calcein released relative to 0.1% Triton-X (defined as 100%) from 3:1 DMPC/DMPG, and 1:1 and 3:1 POPC/POPG (mol/mol) liposomes, in presence of aurein 2.2, aurein 2.3, and aurein 2.3-COOH

Peptides	Aurein 2.2			Aurein 2.3			Aurein 2.3-COOH		
P/L ratio	1:15	1:80	1:120	1:15	1:80	1:120	1:15	1:80	1:120
3:1 DMPC/PG	92%			87%			93%		
1:1 POPC/PG	27% ± 2%	4%	2%	18% ± 2%	3%	3%	21% ± 5%	1%	2%
3:1 POPC/PG	36% ± 2%	4%	1%	12% ± 3%	6%	1%	16% ± 5%	1%	2%

Errors associated with measurements were determined for P/L ratio of 1:15 in 1:1 and 3:1 POPC/POPG from repeated measurements, and are given here.

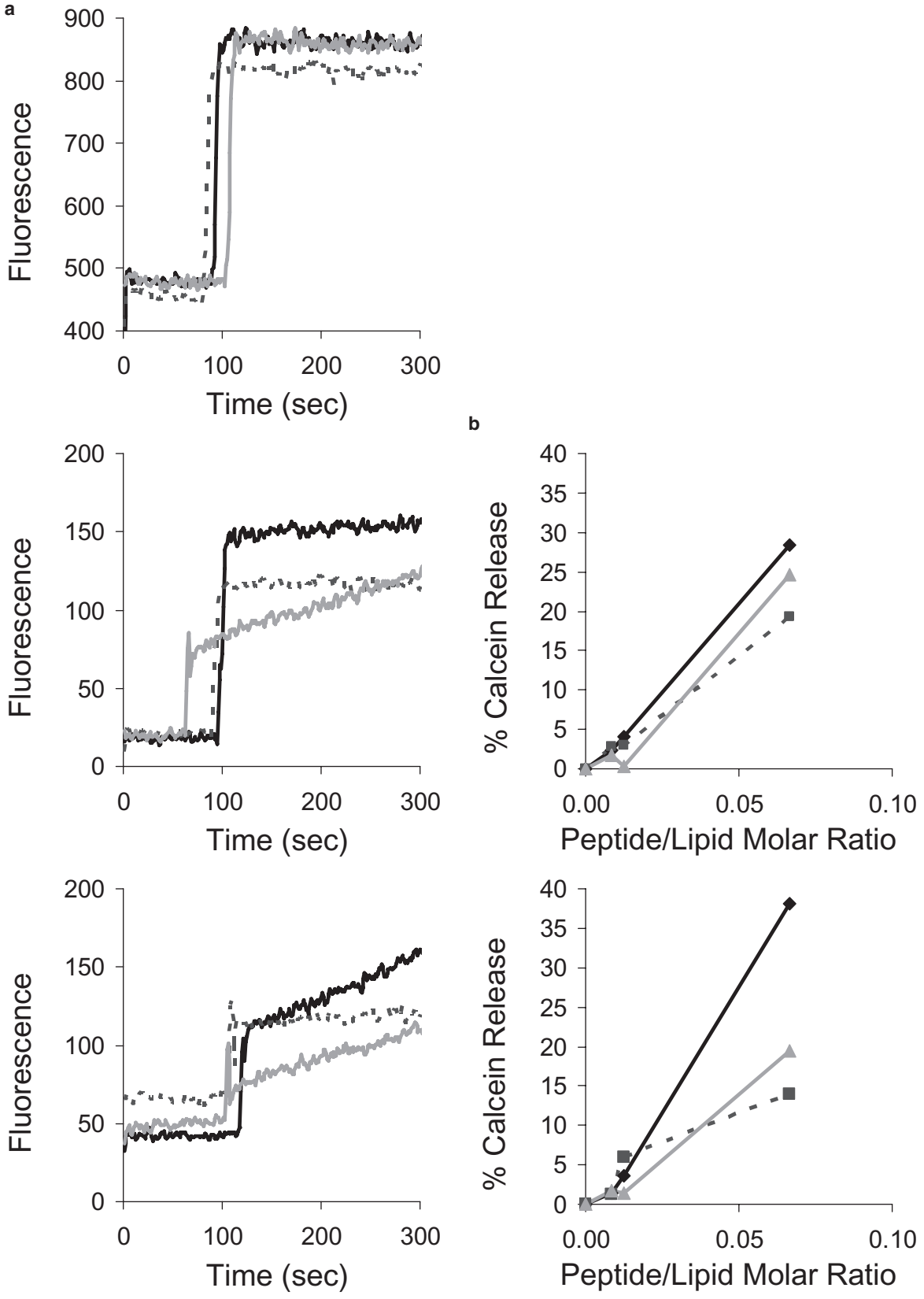
a
Fluorescence
Time (sec)
b
% Calcein Release
Peptide/Lipid Molar Ratio

initially. Fig. 6 *b* shows the concentration dependence of aurein-induced calcein release for 1:1 (*middle*) and 3:1 POPC/POPG (*bottom*) (mol/mol) liposomes. The percentage of calcein released increased as the peptide concentration increased for all aurein peptides. At low peptide concentrations, no difference was evident between peptides within the margin of error (±2–5%) of the experiment.

Aurein-induced membrane leakage in *S. aureus*, using $DiSC_35$ assays

Antimicrobial peptides can kill bacteria through many different mechanisms in which cytoplasmic membrane depolarization is a common target site. To observe the effects of aurein peptides on the cytoplasmic membrane of *S. aureus* C622, we performed membrane-depolarization experiments using the membrane-sensitive dye $DiSC_35$. All peptides were compared with the membrane perturbing cyclic peptide gramicidin S. Fig. 7 shows that at 1–5 times the MIC, aurein 2.2 demonstrated greater depolarization of the membrane than any of the other peptides, including gramicidin S. Aurein 2.3 demonstrated similar depolarization to gramicidin S at 1 × MIC, whereas aurein 2.3-COOH was much less efficient than gramicidin S. Increasing the level of aurein peptide added to 5 × MIC showed an increased depolarization affect for both amidated peptides.

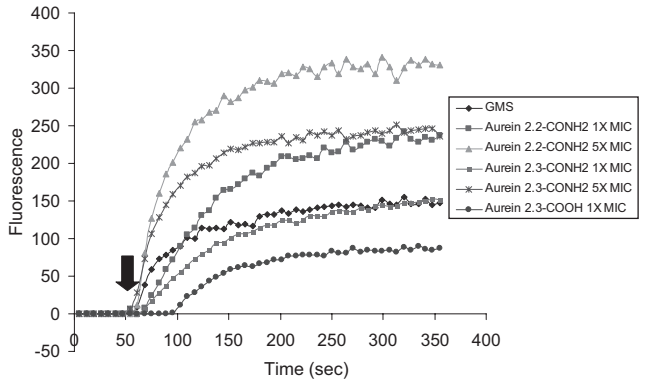

FIGURE 7 Membrane depolarization of *S. aureus* C622 induced by aurein 2.2 at 1 × MIC and 5 × MIC; aurein 2.3 at 1× MIC and 5 × MIC; and aurein 2.3-COOH at 1 × MIC. MIC values are described elsewhere (36). Gramicidin S (1 × MIC) was used as control. Results are representative of 2–3 experiments. Arrow represents time when peptide was added.

DISCUSSION

Understanding how membrane composition modulates peptide-lipid interactions can be an important step in unlocking the mechanism of action of a given antimicrobial peptide. Here, we further examined how two antimicrobial peptides from the Australian southern bell frog *Litoria aurea*, i.e., aurein 2.2 and aurein 2.3, interact with a range of model membranes and the membrane from *S. aureus* C622. As a negative control, we also investigated the peptide-lipid interaction of a nonactive analog, aurein 2.3-COOH.

The bacterial membrane composition varies from bacterium to bacterium, and also as a response to changing environments (68,69) and exposure to antibiotics (70–72). Phosphatidyl-ethanolamine is known as a major membrane component (up to 80%) in Gram-negative bacteria (72–74), whereas PG is identified as a major membrane component (up to 58%) in Gram-positive bacteria (75–78). Incorporating PG in model membranes is thus necessary to replicate the lipid bilayers of Gram-positive bacteria. Previous studies were often conducted in model membranes with a 33% or 50% molar PG content (14,43,64,79–82). The DMPC/DMPG bilayers (19,56,57,64,79,81) and POPC/POPG bilayers (14,19,43,80,83) are the most commonly used bacterial membrane models. Other models include PG only, or mixtures of DOPC/DOPG (84,85) or DPPC/DPPG (57,86,87), to account for different bilayer thicknesses and fluidities. Our study involved the most widely used models, i.e., DMPC/DMPG (~26 Å) (55) and POPC/POPG (~39 Å) (57) bilayers, to determine whether bilayer thickness or PG content exerts an effect on aurein peptide-lipid interactions.

It is widely accepted that cationic antimicrobial peptides only adopt secondary structures in the presence of membranes (1,58,88), and that the adoption of a secondary structure is a key first step toward membrane interaction. Our solution CD results showed that the structures of the three aurein peptides were similar in the presence of 1:1 DMPC/DMPG (36) and, as demonstrated here, in 3:1 DMPC/DMPG. Maculatin 1.1 and citropin 1.1, α-helical antimicrobial peptides from tree frogs, were also shown to retain their structures in DMPC, DMPG, POPC, and POPG membranes (19,89). We demonstrated here, however, that helical content depends on membrane bilayer thickness, with differences in percent α-helical structure between DMPC/DMPG and POPC/POPG. This finding demonstrates that secondary structure is independent of PG content, but depends on bilayer thickness. In other words, membrane bilayer thickness appears to have an effect on the ability of a peptide to bind the membrane and, consequently, to have an effect on the ability of a lipid bilayer to induce peptide secondary structures.

Many studies demonstrated how electrostatics and bilayer thickness play an important role in peptide-lipid

FIGURE 6 (*a*) Calcein release spectra of 3:1 DMPC/DMPG (mol/mol) (*top*), and 1:1 (*middle*) and 3:1 POPC/POPG (mol/mol) (*bottom*) SUVs in the presence of aurein 2.2 (*black solid line*), aurein 2.3 (*black dotted line*), and aurein 2.3-COOH (*gray solid line*) at a 1:15 peptide/lipid molar ratio. (*b*) Percentage of calcein released from 1:1 (*top*) and 3:1 POPC/POPG (mol/mol) (*bottom*) SUVs in the presence of aurein 2.2 (*black solid line*), aurein 2.3 (*black dotted line*), and aurein 2.3-COOH (*gray solid line*) as a function of peptide/lipid molar ratio.

interactions (14,43–45,64,90). In the latter case, it was generally shown that longer antimicrobial peptides, e.g., caerin 1.1 and maculatin 1.1 (19), insert more readily into lipid bilayers, and undergo less impact from increased bilayer thickness. On the other hand, shorter antimicrobial peptides insert less readily, and compensate by inserting into only one leaflet, or by tilting to minimize hydrophobic mismatch. In addition, it was recently shown that the tilt of helices, which increases with decreasing bilayer thickness and has an impact on the ability of a peptide to oligomerize (91), is not necessarily accompanied by a change in the phase, order, or structure of lipid bilayers (92). In this study, a clear difference in the insertion profile of aurein peptides was observed as a function of bilayer thickness. In the thinner DMPC/DMPG bilayers, much lower concentrations of amidated peptides were required for insertion (P/L, ~1:200 for 1:1 DMPC/DMPG). In POPC/POPG bilayers, higher aurein peptide concentrations were required to produce a change from the surface-adsorbed state to the inserted or tilted state. From a different view, one might argue that the thinner DMPC/DMPG membranes result in a larger portion of peptides interacting with the entire lipid molecules (headgroups and chains), resulting in more membrane disruption, as shown in Fig. 8 *a*, and as evidenced by the ^{31}P NMR, DSC, and calcein data. In the case of POPC/POPG membranes (Fig. 8 *b*), aurein peptides may be forced to interact comparatively more with the surface, resulting in a toroidal pore or related (i.e., distorted toroidal or localized membrane aggregate) mechanism, where the lipid headgroups are perturbed (as seen in the ^{31}P NMR data), but not the lipid acyl chains (as seen in DSC data). Because many more peptides in this case would be required to line the defects in the membrane bilayers (15,58–61), the amount of calcein released for a given P/L ratio should be lower than in a case where micellerization occurs (Fig. 8).

In terms of electrostatics, the increase in the amount of PG in DMPC/DMPG bilayers clearly has the effect that fewer peptides are required to promote insertion into the membrane. Indeed, the threshold P/L ratio in 1:1 DMPC/DMPG was ~1:200, whereas in 3:1 DMPC/DMPG, it was between 1:40 and 1:80. Presumably the increased negative charge in 1:1 DMPC/DMPG favored the binding of aurein peptides to the surface, enabling them to insert and perturb the membrane bilayers more readily. In the case of POPC/POPG, the increased negative charge in the case of 1:1 vs. 3:1 resulted in a more complex effect and insertion profile. Here, the increased PG content had the effect of differentiating the behavior of aurein 2.2 from that of aurein 2.3 and from that of aurein 2.3-COOH. Presumably in the case of POPC/POPG, where distorted toroidal pores or localized membrane aggregates might be formed, and peptides might pack (or aggregate?) to line these defects, not only would peptide-lipid electrostatic interactions be important, but also peptide-peptide electrostatic interactions. A number of studies showed that Leu is more hydrophobic in peptides than Ile (93–96), suggesting that aurein 2.2 would more likely aggregate. To verify whether aurein 2.2 is more likely to form oligomers in solution, the retention times of aurein 2.2 and aurein 2.3 on a reverse-phase high-performance liquid chromatography were determined. Pure peptides were injected and eluted under a gradient of water/acetonitrile, as used to purify the crude peptides (see Materials and Methods). The retention times for both peptides were nearly identical, indicating that both peptides behave the same way in solution. To probe further whether aurein 2.2 has a higher propensity to oligomerize in membranes, nuclear Overhauser effect spectroscopy (NOESY) spectra were

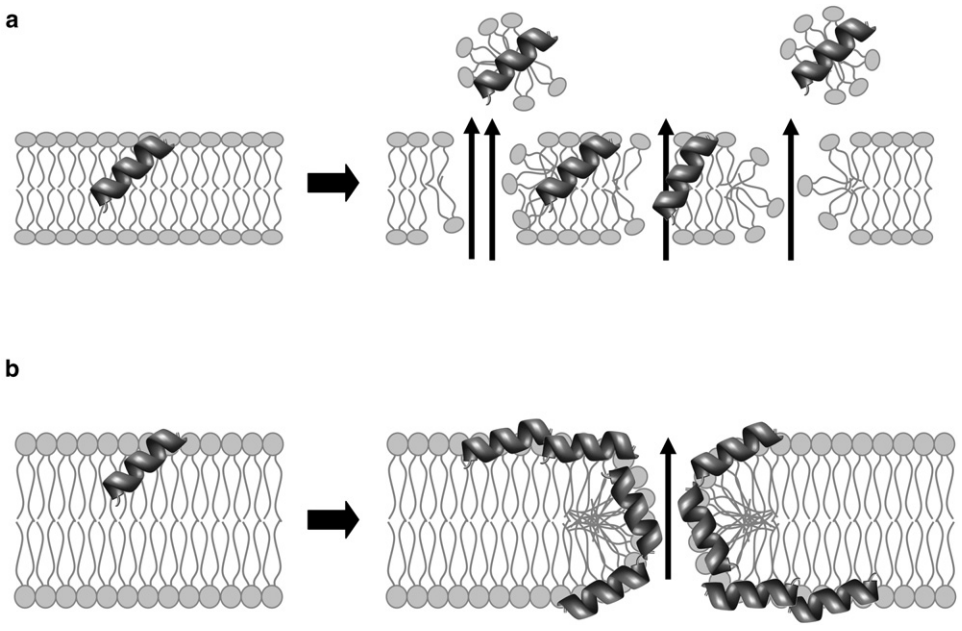

FIGURE 8 General model for perturbation of (*a*) DMPC/DMPG and (*b*) POPC/POPG by aurein peptides. To keep the model simple, some finer points, such as distinction in ability of aurein 2.2 to induce membrane depolarization in *S. aureus* C622 compared with aurein 2.3 and aurein 2.3-COOH, are obviously not taken into account. Arrows represent leakage.

acquired for aurein 2.2 in dodecylphosphocholine (DPC) micelles, and for aurein 2.3 under the same conditions. Preliminary data suggests that aurein 2.2 forms dimers in DPC micelles, because of the larger number of long-range NOE crosspeaks found, as reported for MSI-78 (37).

A comparison of calcein-release and $DiSC_35$ data clearly shows the merits and limitations of using model membranes. By using the same model membranes in the calcein release assay as in the other experiments (OCD, ^{31}P NMR, and DSC), a comprehensive model of the interactions of aurein peptides with well-defined DMPC/DMPG and POPC/POPG membranes can be elucidated. For instance, the calcein data clearly show that all three aurein peptides are equally efficient at perturbing 3:1 DMPC/DMPG liposomes, a finding supported by the OCD, ^{31}P NMR, and DSC data. The calcein release data also demonstrate that aurein 2.2 is better at inducing leakage at high concentrations, compared with the other two peptides, a finding supported by the $DiSC_35$ data. On the other hand, the calcein data suggest that the inactive aurein 2.3-COOH is more efficient at perturbing both 1:1 and 3:1 POPC/POPG liposomes than the amidated version, a finding clearly unsupported by much of the other data, and especially by the biological data, which are consistent with the inactivity of this peptide.

Overall, the results presented here suggest that aurein peptides interact with membranes in a manner that is dependent on lipid composition and on sequence. The $DiSC_35$ data show that aurein 2.2 is better at inducing membrane depolarization than aurein 2.3, which is itself as efficient as gramicidin S. The OCD data of the three peptides in the 1:1 POPC/POPG model membranes show similar distinction in the behavior of the peptides, suggesting that perhaps this lipid composition is optimal for studying this subset of the aurein peptide family. Finally, if one assumes that the 1:1 POPC/POPG membranes are the most relevant, and that the peptides function by inducing distorted toroidal pores or localized membrane aggregates, then the sequence dependence observed in the $DiSC_35$ results may be related to differences in the potential of aurein 2.2 to form oligomers relative to the other two peptides, but only in the membrane.

SUPPORTING MATERIAL

A table, references, and two figures are available at http://www.biophysj.org/biophysj/supplemental/S0006-3495(08)00066-0.

The authors thank Fred Rossell and Louise Creagh of the Laboratory of Molecular Biophysics hubs, for their help in maintaining the CD and calorimetry instrumentation, respectively.

J.D.H. and R.E.W.H. acknowledge funding from the Advanced Food and Materials Network. J.D.H. received a Canadian Commonwealth Post-Doctoral Research Fellowship. S.K.S. gratefully acknowledges the support of the National Sciences and Engineering Research Council of Canada through a Discovery Grant, and the Michael Smith Foundation for Health Research through a Career Investigator Award. R.E.W.H. was funded by Canadian Institutes of Health Research, and is the recipient of a Canada Research Chair.

REFERENCES

1. Hancock, R. E. W. 2001. Cationic peptides: effectors in innate immunity and novel antimicrobials. *Lancet Infect. Dis.* 1:156–164.
2. Hancock, R. E. W. 2005. Mechanisms of action of newer antibiotics for Gram-positive pathogens. *Lancet Infect. Dis.* 5:209–218.
3. Devine, D. A., and R. E. W. Hancock. 2002. Cationic peptides: distribution and mechanisms of resistance. *Curr. Pharm. Des.* 8:703–714.
4. Pukala, T. L., J. H. Bowie, V. M. Maselli, I. F. Musgrave, and M. J. Tyler. 2006. Host-defence peptides from the glandular secretions of amphibians: structure and activity. *Nat. Prod. Rep.* 23:368–393.
5. Rinaldi, A. C. 2002. Antimicrobial peptides from amphibian skin: an expanding scenario. *Curr. Opin. Chem. Biol.* 6:799–804.
6. Giovannini, M. G., L. Poulter, B. W. Gibson, and D. H. Williams. 1987. Biosynthesis and degradation of peptides derived from *Xenopus laevis* prohormones. *Biochem. J.* 243:113–120.
7. Zasloff, M. 1987. Magainins, a class of antimicrobial peptides from *Xenopus* skin: isolation, characterization of two active forms, and partial cDNA sequence of a precursor. *Proc. Natl. Acad. Sci. USA.* 84:5449–5453.
8. Zasloff, M., B. Martin, and H. C. Chen. 1988. Antimicrobial activity of synthetic magainin peptides and several analogues. *Proc. Natl. Acad. Sci. USA.* 85:910–913.
9. Bechinger, B. 2005. Detergent-like properties of magainin antibiotic peptides: a ^{31}P solid-state NMR spectroscopy study. *Biochim. Biophys. Acta.* 1712:101–108.
10. Bechinger, B., M. Zasloff, and S. J. Opella. 1993. Structure and orientation of the antibiotic peptide magainin in membranes by solid-state nuclear magnetic resonance spectroscopy. *Protein Sci.* 2:2077–2084.
11. Duclohier, H., G. Molle, and G. Spach. 1989. Antimicrobial peptide magainin I from *Xenopus* skin forms anion-permeable channels in planar lipid bilayers. *Biophys. J.* 56:1017–1021.
12. Hallock, K. J., D. K. Lee, and A. Ramamoorthy. 2003. MSI-78, an analogue of the magainin antimicrobial peptides, disrupts lipid bilayer structure via positive curvature strain. *Biophys. J.* 84:3052–3060.
13. Jacob, L., and M. Zasloff. 1994. Potential therapeutic applications of magainins and other antimicrobial agents of animal origin. *Ciba Found. Symp.* 186:197–223.
14. Ramamoorthy, A., S. Thennarasu, D. K. Lee, A. Tan, and L. Maloy. 2006. Solid-state NMR investigation of the membrane-disrupting mechanism of antimicrobial peptides MSI-78 and MSI-594 derived from magainin 2 and melittin. *Biophys. J.* 91:206–216.
15. Yang, L., T. M. Weiss, R. I. Lehrer, and H. W. Huang. 2000. Crystallization of antimicrobial pores in membranes: magainin and protegrin. *Biophys. J.* 79:2002–2009.
16. Ambroggio, E. E., F. Separovic, J. Bowie, and G. D. Fidelio. 2004. Surface behaviour and peptide-lipid interactions of the antibiotic peptides. *Maculatin and Citropin. Biochim Biophys Acta.* 1664:31–37.
17. Ambroggio, E. E., F. Separovic, J. H. Bowie, G. D. Fidelio, and L. A. Bagatolli. 2005. Direct visualization of membrane leakage induced by the antibiotic peptides: maculatin, citropin, and aurein. *Biophys. J.* 89:1874–1881.
18. Balla, M. S., J. H. Bowie, and F. Separovic. 2004. Solid-state NMR study of antimicrobial peptides from Australian frogs in phospholipid membranes. *Eur. Biophys. J.* 33:109–116.
19. Marcotte, I., K. L. Wegener, Y. H. Lam, B. C. Chia, M. R. de Planque, et al. 2003. Interaction of antimicrobial peptides from Australian amphibians with lipid membranes. *Chem. Phys. Lipids.* 122:107–120.
20. Niidome, T., K. Kobayashi, H. Arakawa, T. Hatakeyama, and H. Aoyagi. 2004. Structure-activity relationship of an antibacterial peptide, maculatin 1.1, from the skin glands of the tree frog, *Litoria genimaculata*. *J. Pept. Sci.* 10:414–422.

21. Boland, M. P., and F. Separovic. 2006. Membrane interactions of antimicrobial peptides from Australian tree frogs. *Biochim. Biophys. Acta.* 1758:1178–1183.

22. Chen, T., L. Li, M. Zhou, P. Rao, B. Walker, et al. 2006. Amphibian skin peptides and their corresponding cDNAs from single lyophilized secretion samples: identification of novel brevinins from three species of Chinese frogs. *Peptides.* 27:42–48.

23. Conlon, J.M., N. Al-Ghaferi, B. Abraham, H. Jiansheng, P. Cosette, et al. 2006. Antimicrobial peptides from diverse families isolated from the skin of the Asian frog, *Rana grahami*. *Peptides.*27:2111–2117.

24. Kumari, V. K., and R. Nagaraj. 2001. Structure-function studies on the amphibian peptide brevinin 1E: translocating the cationic segment from the C-terminal end to a central position favors selective antibacterial activity. *J. Pept. Res.* 58:433–441.

25. Morikawa, N., K. Hagiwara, and T. Nakajima. 1992. Brevinin-1 and -2, unique antimicrobial peptides from the skin of the frog, *Rana brevipoda porsa*. *Biochem. Biophys. Res. Commun.* 189:184–190.

26. Simmaco, M., G. Mignogna, D. Barra, and F. Bossa. 1993. Novel antimicrobial peptides from skin secretion of the European frog *Rana esculenta*. *FEBS Lett.* 324:159–161.

27. Won, H. S., S. S. Kim, S. J. Jung, W. S. Son, B. Lee, et al. 2004. Structure-activity relationships of antimicrobial peptides from the skin of *Rana esculenta* inhabiting Korea. *Mol. Cells.* 17:469–476.

28. Apponyi, M. A., T. L. Pukala, C. S. Brinkworth, V. M. Maselli, J. H. Bowie, et al. 2004. Host-defence peptides of Australian anurans: structure, mechanism of action and evolutionary significance. *Peptides.* 25:1035–1054.

29. Rozek, T., J. H. Bowie, J. C. Wallace, and M. J. Tyler. 2000. The antibiotic and anticancer active aurein peptides from the Australian bell frogs *Litoria aurea* and *Litoria raniformis*. Part 2. Sequence determination using electrospray mass spectrometry. *Rapid Commun. Mass Spectrom.* 14:2002–2011.

30. Rozek, T., K. L. Wegener, J. H. Bowie, I. N. Olver, J. A. Carver, et al. 2000. The antibiotic and anticancer active aurein peptides from the Australian bell frogs *Litoria aurea* and *Litoria raniformis* the solution structure of aurein 1.2. *Eur. J. Biochem.* 267:5330–5341.

31. Wang, G., Y. Li, and X. Li. 2005. Correlation of three-dimensional structures with the antibacterial activity of a group of peptides designed based on a nontoxic bacterial membrane anchor. *J. Biol. Chem.* 280:5803–5811.

32. Giacometti, A., O. Cirioni, A. Riva, W. Kamysz, C. Silvestri, et al. 2007. In vitro activity of aurein 1.2 alone and in combination with antibiotics against Gram-positive nosocomial cocci. *Antimicrob. Agents Chemother.* 51:1494–1496.

33. Vaara, M., and M. Porro. 1996. Group of peptides that act synergistically with hydrophobic antibiotics against Gram-negative enteric bacteria. *Antimicrob. Agents Chemother.* 40:1801–1805.

34. McCafferty, D. G., P. Cudic, M. K. Yu, D. C. Behenna, and R. Kruger. 1999. Synergy and duality in peptide antibiotic mechanisms. *Curr. Opin. Chem. Biol.* 3:672–680.

35. Seto, G. W., S. Marwaha, D. M. Kobewka, R. N. Lewis, F. Separovic, et al. 2007. Interactions of the Australian tree frog antimicrobial peptides aurein 1.2, citropin 1.1 and maculatin 1.1 with lipid model membranes: differential scanning calorimetric and Fourier transform infrared spectroscopic studies. *Biochim. Biophys. Acta.* 1768:2787–2800.

36. Pan, Y. L., J. T. Cheng, J. Hale, J. Pan, R. E. Hancock, et al. 2007. Characterization of the structure and membrane interaction of the antimicrobial peptides aurein 2.2 and 2.3 from Australian southern bell frogs. *Biophys. J.* 92:2854–2864.

37. Porcelli, F., B. A. Buck-Koehntop, S. Thennarasu, A. Ramamoorthy, and G. Veglia. 2006. Structures of the dimeric and monomeric variants of magainin antimicrobial peptides (MSI-78 and MSI-594) in micelles and bilayers, determined by NMR spectroscopy. *Biochemistry.* 45:5793–5799.

38. Wu, Y., K. He, S. J. Ludtke, and H. W. Huang. 1995. X-ray diffraction study of lipid bilayer membranes interacting with amphiphilic helical peptides: diphytanoyl phosphatidylcholine with alamethicin at low concentrations. *Biophys. J.* 68:2361–2369.

39. Dave, P. C., E. Billington, Y. L. Pan, and S. K. Straus. 2005. Interaction of alamethicin with ether-linked phospholipid bilayers: oriented circular dichroism, ^{31}P solid-state NMR, and differential scanning calorimetry studies. *Biophys. J.* 89:2434–2442.

40. Harzer, U., and B. Bechinger. 2000. Alignment of lysine-anchored membrane peptides under conditions of hydrophobic mismatch: a CD, ^{15}N and ^{31}P solid-state NMR spectroscopy investigation. *Biochemistry.* 39:13106–13114.

41. Tremouilhac, P., E. Strandberg, P. Wadhwani, and A.S. Ulrich. 2006. Synergistic transmembrane alignment of the antimicrobial heterodimer PGLa/magainin 2. *J. Biol. Chem.* 281:32089–32094.

42. Bechinger, B., and K. Lohner. 2006. Detergent-like actions of linear amphipathic cationic antimicrobial peptides. *Biochim. Biophys. Acta.* 1758:1529–1539.

43. Dathe, M., H. Nikolenko, J. Meyer, M. Beyermann, and M. Bienert. 2001. Optimization of the antimicrobial activity of magainin peptides by modification of charge. *FEBS Lett.* 501:146–150.

44. Wieprecht, T., M. Dathe, E. Krause, M. Beyermann, W. L. Maloy, et al. 1997. Modulation of membrane activity of amphipathic, antibacterial peptides by slight modifications of the hydrophobic moment. *FEBS Lett.* 417:135–140.

45. Dathe, M., H. Nikolenko, J. Klose, and M. Bienert. 2004. Cyclization increases the antimicrobial activity and selectivity of arginine- and tryptophan-containing hexapeptides. *Biochemistry.* 43:9140–9150.

46. Hilpert, K., M. R. Elliott, R. Volkmer-Engert, P. Henklein, O. Donini, et al. 2006. Sequence requirements and an optimization strategy for short antimicrobial peptides. *Chem. Biol.* 13:1101–1107.

47. Lewis, R. N., F. Liu, R. Krivanek, P. Rybar, T. Hianik, et al. 2007. Studies of the minimum hydrophobicity of alpha-helical peptides required to maintain a stable transmembrane association with phospholipid bilayer membranes. *Biochemistry.* 46:1042–1054.

48. Moll, F., 3rd, and T. A. Cross. 1990. Optimizing and characterizing alignment of oriented lipid bilayers containing gramicidin D. *Biophys. J.* 57:351–362.

49. Hallock, K. J., K. Henzler Wildman, D. K. Lee, and A. Ramamoorthy. 2002. An innovative procedure using a sublimable solid to align lipid bilayers for solid-state NMR studies. *Biophys. J.* 82:2499–2503.

50. Johnson, W. C. 1999. Analyzing protein circular dichroism spectra for accurate secondary structures. *Proteins.* 35:307–312.

51. Provencher, S. W., and J. Glockner. 1981. Estimation of globular protein secondary structure from circular dichroism. *Biochemistry.* 20:33–37.

52. Sreerama, N., S. Y. Venyaminov, and R. W. Woody. 1999. Estimation of the number of alpha-helical and beta-strand segments in proteins using circular dichroism spectroscopy. *Protein Sci.* 8:370–380.

53. Sreerama, N., and R. W. Woody. 1994. Protein secondary structure from circular dichroism spectroscopy. Combining variable selection principle and cluster analysis with neural network, ridge regression and self-consistent methods. *J. Mol. Biol.* 242:497–507.

54. Sreerama, N., and R. W. Woody. 1993. A self-consistent method for the analysis of protein secondary structure from circular dichroism. *Anal. Biochem.* 209:32–44.

55. Kucerka, N., M. A. Kiselev, and P. Balgavy. 2004. Determination of bilayer thickness and lipid surface area in unilamellar dimyristoylphosphatidylcholine vesicles from small-angle neutron scattering curves: a comparison of evaluation methods. *Eur. Biophys. J.* 33:328–334.

56. Mecke, A., D. K. Lee, A. Ramamoorthy, B. G. Orr, and M. M. Banaszak Holl. 2005. Membrane thinning due to antimicrobial peptide binding: an atomic force microscopy study of MSI-78 in lipid bilayers. *Biophys. J.* 89:4043–4050.

57. Leidy, C., L. Linderoth, T. L. Andresen, O. G. Mouritsen, K. Jorgensen, et al. 2006. Domain-induced activation of human phospholipase A2 type IIA: local versus global lipid composition. *Biophys. J.* 90: 3165–3175.

58. Shai, Y. 1999. Mechanism of the binding, insertion and destabilization of phospholipid bilayer membranes by alpha-helical antimicrobial and cell non-selective membrane-lytic peptides. *Biochim. Biophys. Acta.* 1462:55–70.

59. Papo, N., and Y. Shai. 2005. Host defense peptides as new weapons in cancer treatment. *Cell. Mol. Life Sci.* 62:784–790.

60. Matsuzaki, K. 1999. Why and how are peptide-lipid interactions utilized for self-defense? Magainins and tachyplesins as archetypes. *Biochim. Biophys. Acta.* 1462:1–10.

61. Huang, H. W. 2000. Action of antimicrobial peptides: two-state model. *Biochemistry.* 39:8347–8352.

62. Wu, M., E. Maier, R. Benz, and R. E. W. Hancock. 1999. Mechanism of interaction of different classes of cationic antimicrobial peptides with planar bilayers and with the cytoplasmic membrane of *Escherichia coli*. *Biochemistry.* 38:7235–7242.

63. Hancock, R. E. W., and D. S. Chapple. 1999. Peptide antibiotics. *Antimicrob. Agents Chemother.* 43:1317–1323.

64. Henzler-Wildman, K. A., G. V. Martinez, M. F. Brown, and A. Ramamoorthy. 2004. Perturbation of the hydrophobic core of lipid bilayers by the human antimicrobial peptide LL-37. *Biochemistry.* 43:8459–8469.

65. Buffy, J. J., M. J. McCormick, S. Wi, A. Waring, R. I. Lehrer, et al. 2004. Solid-state NMR investigation of the selective perturbation of lipid bilayers by the cyclic antimicrobial peptide RTD-1. *Biochemistry.* 43:9800–9812.

66. Mani, R., J. J. Buffy, A. J. Waring, R. I. Lehrer, and M. Hong. 2004. Solid-state NMR investigation of the selective disruption of lipid membranes by protegrin-1. *Biochemistry.* 43:13839–13848.

67. Jung, D., J.P. Powers, S.K. Straus, and R.E. Hancock. 2008. Lipid-specific binding of the calcium-dependent antibiotic daptomycin leads to changes in lipid polymorphism of model membranes. *Chem. Phys. Lipids.* 154:120–128.

68. Frerman, F. E., and D. C. White. 1967. Membrane lipid changes during formation of a functional electron transport system in *Staphylococcus aureus*. *J. Bacteriol.* 94:1868–1874.

69. Joyce, G. H., R. K. Hammond, and D. C. White. 1970. Changes in membrane lipid composition in exponentially growing *Staphylococcus aureus* during the shift from 37 to 25°C. *J. Bacteriol.* 104:323–330.

70. Appelbaum, P. C., and B. Bozdogan. 2004. Vancomycin resistance in *Staphylococcus aureus*. *Clin. Lab. Med.* 24:381–402.

71. Bozdogan, B., D. Esel, C. Whitener, F. A. Browne, and P. C. Appelbaum. 2003. Antibacterial susceptibility of a vancomycin-resistant *Staphylococcus aureus* strain isolated at the Hershey Medical Center. *J. Antimicrob. Chemother.* 52:864–868.

72. Conrad, R. S., and H. E. Gilleland, Jr. 1981. Lipid alterations in cell envelopes of polymyxin-resistant *Pseudomonas aeruginosa* isolates. *J. Bacteriol.* 148:487–497.

73. Gmeiner, J., and H. H. Martin. 1976. Phospholipid and lipopolysaccharide in *Proteus mirabilis* and its stable protoplast L-form. Difference in content and fatty acid composition. *Eur. J. Biochem.* 67:487–494.

74. Morein, S., A. Andersson, L. Rilfors, and G. Lindblom. 1996. Wild-type *Escherichia coli* cells regulate the membrane lipid composition in a "window" between gel and non-lamellar structures. *J. Biol. Chem.* 271:6801–6809.

75. Clejan, S., T. A. Krulwich, K. R. Mondrus, and D. Seto-Young. 1986. Membrane lipid composition of obligately and facultatively alkalophilic strains of *Bacillus* spp. *J. Bacteriol.* 168:334–340.

76. Beining, P. R., E. Huff, B. Prescott, and T. S. Theodore. 1975. Characterization of the lipids of mesosomal vesicles and plasma membranes from *Staphylococcus aureus*. *J. Bacteriol.* 121:137–143.

77. Trombe, M. C., M. A. Laneelle, and G. Laneelle. 1979. Lipid composition of aminopterin-resistant and sensitive strains of *Streptococcus pneumoniae*. Effect of aminopterin inhibition. *Biochim. Biophys. Acta.* 574:290–300.

78. Haque, M. A., and N. J. Russell. 2004. Strains of *Bacillus cereus* vary in the phenotypic adaptation of their membrane lipid composition in response to low water activity, reduced temperature and growth in rice starch. *Microbiology.* 150:1397–1404.

79. Lewis, R. N., Y. P. Zhang, and R. N. McElhaney. 2005. Calorimetric and spectroscopic studies of the phase behavior and organization of lipid bilayer model membranes composed of binary mixtures of dimyristoylphosphatidylcholine and dimyristoylphosphatidylglycerol. *Biochim. Biophys. Acta.* 1668:203–214.

80. Yamaguchi, S., D. Huster, A. Waring, R. I. Lehrer, W. Kearney, et al. 2001. Orientation and dynamics of an antimicrobial peptide in the lipid bilayer by solid-state NMR spectroscopy. *Biophys. J.* 81:2203–2214.

81. Chekmenev, E. Y., B. S. Vollmar, K. T. Forseth, M. N. Manion, S. M. Jones, et al. 2006. Investigating molecular recognition and biological function at interfaces using piscidins, antimicrobial peptides from fish. *Biochim. Biophys. Acta.* 1758:1359–1372.

82. Epand, R. F., P. B. Savage, and R. M. Epand. 2007. Bacterial lipid composition and the antimicrobial efficacy of cationic steroid compounds (ceragenins). *Biochim. Biophys. Acta.* 1768:2500–2509.

83. Lu, J. X., K. Damodaran, J. Blazyk, and G. A. Lorigan. 2005. Solid-state nuclear magnetic resonance relaxation studies of the interaction mechanism of antimicrobial peptides with phospholipid bilayer membranes. *Biochemistry.* 44:10208–10217.

84. Wimmer, R., K. K. Andersen, B. Vad, M. Davidsen, S. Molgaard, et al. 2006. Versatile interactions of the antimicrobial peptide novispirin with detergents and lipids. *Biochemistry.* 45:481–497.

85. Epand, R. F., M. A. Schmitt, S. H. Gellman, and R. M. Epand. 2006. Role of membrane lipids in the mechanism of bacterial species selective toxicity by two alpha/beta-antimicrobial peptides. *Biochim. Biophys. Acta.* 1758:1343–1350.

86. Klajnert, B., J. Janiszewska, Z. Urbanczyk-Lipkowska, M. Bryszewska, and R. M. Epand. 2006. DSC studies on interactions between low molecular mass peptide dendrimers and model lipid membranes. *Int. J. Pharm.* 327:145–152.

87. Zweytick, D., G. Pabst, P. M. Abuja, A. Jilek, S. E. Blondelle, et al. 2006. Influence of *N*-acylation of a peptide derived from human lactoferricin on membrane selectivity. *Biochim. Biophys. Acta.* 1758:1426–1435.

88. Zasloff, M. 2002. Antimicrobial peptides in health and disease. *N. Engl. J. Med.* 347:1199–1200.

89. Wegener, K. L., P. A. Wabnitz, J. A. Carver, J. H. Bowie, B. C. Chia, et al. 1999. Host defence peptides from the skin glands of the Australian blue mountains tree-frog *Litoria citropa*. Solution structure of the antibacterial peptide citropin 1.1. *Eur. J. Biochem.* 265:627–637.

90. Henzler Wildman, K. A., D. K. Lee, and A. Ramamoorthy. 2003. Mechanism of lipid bilayer disruption by the human antimicrobial peptide, LL-37. *Biochemistry.* 42:6545–6558.

91. Ramamoorthy, A., D. K. Lee, J. S. Santos, and K. A. Henzler-Wildman. 2008. Nitrogen-14 solid-state NMR spectroscopy of aligned phospholipid bilayers to probe peptide-lipid interaction and oligomerization of membrane associated peptides. *J. Am. Chem. Soc.* 130: 11023–11029.

92. Ramamoorthy, A., S. K. Kandasamy, D. K. Lee, S. Kidambi, and R. G. Larson. 2007. Structure, topology, and tilt of cell-signaling peptides containing nuclear localization sequences in membrane bilayers determined by solid-state NMR and molecular dynamics simulation studies. *Biochemistry.* 46:965–975.

93. Wimley, W. C., and S. H. White. 1996. Experimentally determined hydrophobicity scale for proteins at membrane interfaces. *Nat. Struct. Biol.* 3:842–848.

94. Bull, H. B., and K. Breese. 1974. Surface tension of amino acid solutions: a hydrophobicity scale of the amino acid residues. *Arch. Biochem. Biophys.* 161:665–670.

95. Guy, H. R. 1985. Amino acid side-chain partition energies and distribution of residues in soluble proteins. *Biophys. J.* 47:61–70.

96. Wilson, K. J., A. Honegger, R. P. Stotzel, and G. J. Hughes. 1981. The behaviour of peptides on reverse-phase supports during high-pressure liquid chromatography. *Biochem. J.* 199:31–41.